

# GLASS AND SILICON FOILS FOR X-RAY SPACE TELESCOPE MIRRORS

<sup>#</sup>M. MIKA, L. PINA\*, M. LANDOVA, O. JANKOVSKY, R. KACEROVSKY, L. SVEDA\*,  
R. HAVLIKOVA\*, R. HUDEC\*\*, V. MARSIKOVA\*\*\*, A. INNEMAN\*\*\*

*Institute of Chemical Technology, Technicka 5, Prague, Czech Republic*

*\*Czech Technical University, Faculty of Nuclear Sciences, Brehova 7, Prague, Czech Republic*

*\*\*Astronomical Institute, Academy of Sciences, Fricova 298, Ondrejov, Czech Republic*

*\*\*\*Rigaku Innovative Technologies Europe s.r.o., Novodvorska 994, Prague, Czech Republic*

<sup>#</sup>E-mail: Martin.Mika@vscht.cz

Submitted September 7, 2011; accepted December 6, 2011

**Keywords:** Glass, Silicon, Thermal forming, X-ray

*Unique observations delivered by space X-ray imaging telescopes have been significantly contributing to important discoveries of current astrophysics. The telescopes' most crucial part is a high throughput, heavily nested mirror array reflecting X-rays and focusing them to a detector. Future astronomical projects on large X-ray telescopes require novel materials and technologies for the construction of the reflecting mirrors. The future mirrors must be lightweight and precisely shaped to achieve large collecting area with high angular resolution of a few arc sec. The new materials and technologies must be cost-effective as well. Currently, the most promising materials are glass or silicon foils which are commercially produced on a large scale. A thermal forming process was used for the precise shaping of these foils. The forced and free slumping of the foils was studied in the temperature range of hot plastic deformation and the shapes obtained by the different slumping processes were compared. The shapes and the surface quality of the foils were measured by a Taylor Hobson contact profilometer, a ZYGO interferometer and Atomic Forced Microscopy. In the experiments, both heat-treatment temperature and time were varied following our experiment design. The obtained data and relations can be used for modelling and optimizing the thermal forming procedure.*

## INTRODUCTION

For the last three decades of X-ray astronomy, observations delivered by imaging X-ray telescopes have significantly contributed to important discoveries of current astrophysics [1-5]. Nowadays, there are new projects on high-resolution imaging telescopes with large collecting areas that require lightweight optics allowing multiple nesting with angular resolution below 5 arcsec. The officials of ESA/NASA/JAXA collaborative space project on the International X-Ray Observatory (IXO) have given preferences to cost-effective materials and technologies for the construction of the mirrors [6]. Currently, the most promising materials are thin glass or Si foils that are commercially available with very low micro-roughness [7-13]. We focused on the development and optimization of thermal forming technology with the aim of precisely shaping the foils so that they can fit the more commonly used Wolter-I geometry (Figure 1) [14] while keeping their surface micro-roughness sufficiently low [15-17]. To satisfy the demanding construction parameters, we must precisely control the forming process, which requires the deep understanding of relations between thermal forming conditions and the parameters of the produced optical components for X-ray reflecting mirrors.

## EXPERIMENTAL

### Free slumping of glass

In our forming experiments, we used commercial borosilicate glass Desag D263 that is produced by Schott company [18]. The glass is produced with a very low micro-roughness of only few 0.1 nm. It exhibited a high chemical durability, and its density was 2.51 g cm<sup>-3</sup>. We thermally formed thin glass foils of rectangular shape 75 × 25 × 0.75 mm or 200 × 100 × 0.4 mm. Before the forming experiment, we placed a glass foil on a supporting mandrel with concave surface of radius  $r = 122.3$  mm, as it is illustrated in Figure 2. For the mandrel, we developed a special composite material which prevents sticking of the foil to the mandrel at high temperatures. Then, the foil was heated in an electric furnace from room temperature up to temperatures slightly above the glass transition temperature  $T_g = 557^\circ\text{C}$ . At these constant temperatures the foil was sagging under its own weight. When we are above  $T_g$ , we can form the glass foils by plastic deformation without forming residual mechanical stresses. For the heat treatment, we followed our experiment design and varied the heat-treatment temperature  $T$  from 600 to 660°C, and the heat-treatment time  $t$  from 60 to 90 min. Corresponding glass viscosities

$\eta$  were from  $10^{11.2}$  to  $10^{9.3}$  dPa·s. After the heat treatment, the foil was slowly cooled down to avoid the formation of residual mechanical stresses.

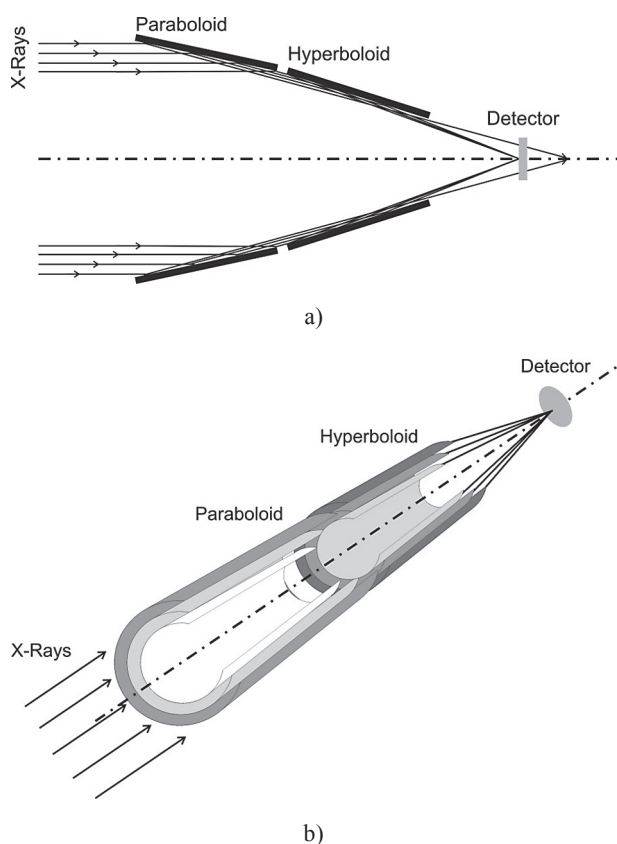


Figure 1. Volter I geometry.

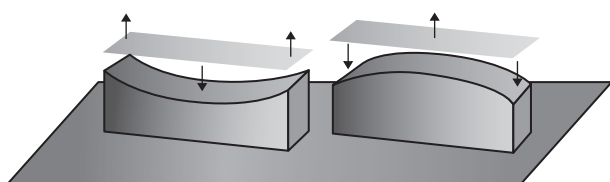


Figure 2. Concave and convex mandrels for glass forming.

#### Forced slumping of glass

For our forced glass slumping experiments, we used the same experimental set up like for the free slumping. In addition, during the heat treatment, we applied vertical force of 0.6 N by placing a convex mandrel on the top surface of a glass foil. In this case,  $T$  varied from 600 to 650°C,  $\eta$  was from  $10^{11.2}$  to  $10^{9.6}$  dPa·s, and  $t$  was from 15 to 60 min.

#### Thermal forming of silicon

For shaping experiments with silicon, we selected 0.6 mm thin monocrystal wafers with the orientation  $\langle 100 \rangle$ . They were doped with B and their electric

resistance was in the range of 325  $\Omega$ . Their density was 2.33 g·cm<sup>-3</sup>. From the wafers, we cut rectangular samples 75 × 25 or 50 × 50 mm. In our approach, we shaped the silicon foils by hot plastic deformation [19, 20]. We placed a silicon foil on a frame consisting of two parallel corundum rods supporting the foil at the edges. Then, we heated the foil above 1000°C, to the region of plastic deformation. The forming process was relatively slow; therefore, we had to apply additional vertical force in the range of 15 N using a cylindrical or a spherical mandrel placed on the top of the silicon foil. To achieve sufficient bending, we kept the foil at high temperature for 60 to 120 min.

#### Metrology

Shapes of the thermally formed samples were measured with a Taylor Hobson PGI PLUS contact profilometer. For each sample, we measured three parallel lines of orthogonal directions; in the centre and close to the edges. Recorded data were processed with Taylor Hobson and Matlab software. Using the profilometer, we also determined surface waviness and micro-roughness of our samples. The surface micro-roughness was also measured with the optical interferometry (ZYGO) and the Atomic Force Microscopy (AFM).

#### RESULTS

By the heat treatment at temperatures above  $T_g$ , we successfully shaped the glass foils by free slumping; an example of the shaped glass foil is shown in Figures 3 and 4. The obtained shapes were close to a parabola, but it was also possible to fit them by circle with peak-to-valley values typically between 10 to 35  $\mu\text{m}$  (Figure 5). For the free slumping of glass foils, the shape was dependent on heat-treatment conditions. To illustrate these effects, we calculated a 3-D plot and a map in Figures 6 and 7 illustrating the effect of  $T$  and  $t$  on the shape radius of glass foils formed by free slumping.

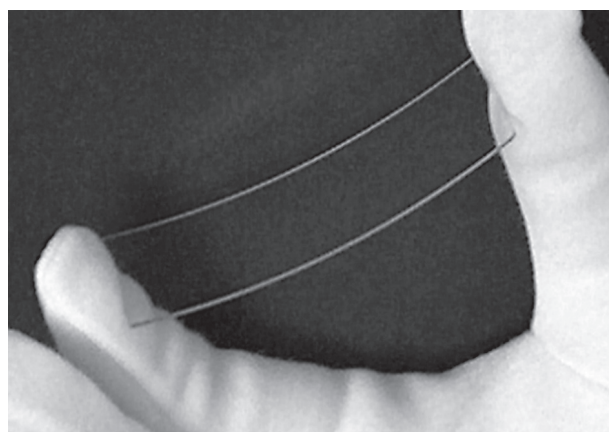


Figure 3. Glass foil 75 × 15 × 0.4 mm formed by forced slumping.

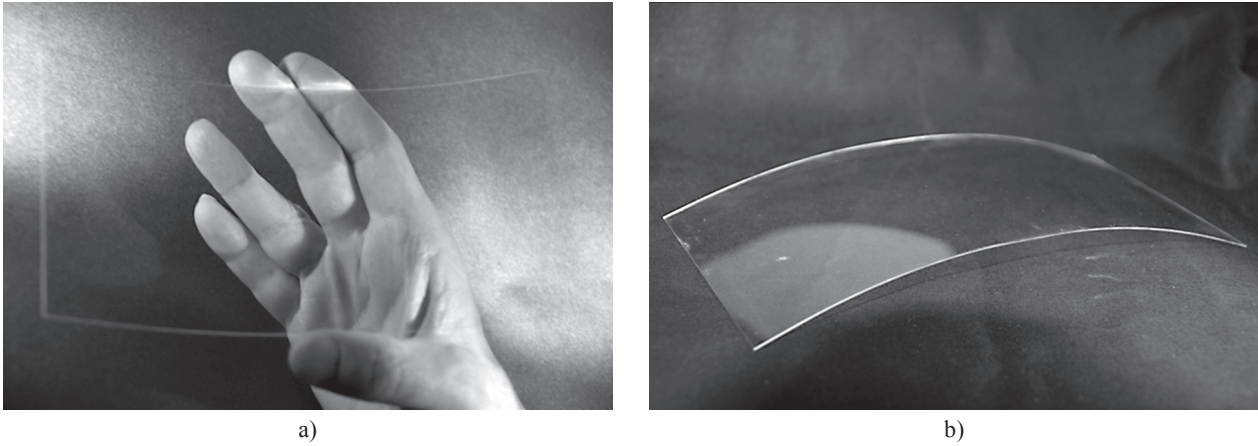


Figure 4. Glass foil 200 × 100 × 0.4 mm formed by free slumping.

For the forced slumping of glass foils, the shape was mostly close to the shape of the mandrel with  $r = 122.3$  mm. In this case, we calculated differences between the radius of the foil and the mandrel. The following 3-D plot and a map in Figures 8 and 9 show how this difference depended on  $T$  and  $t$ . The surface micro-roughness of the glass foils was also influenced by forming conditions. The effect of both  $T$  and  $t$  on the micro-roughness  $R_a$ , measured with the profilometer,

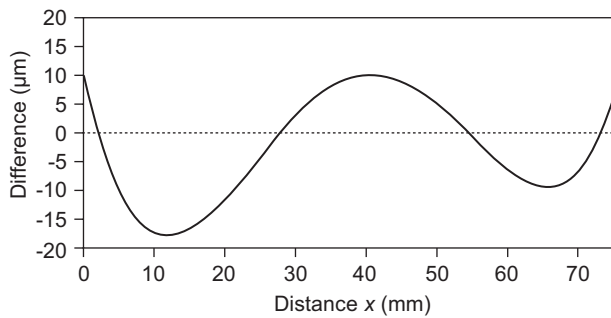


Figure 5. Glass shape deviation from a circle with radius 2033 mm.

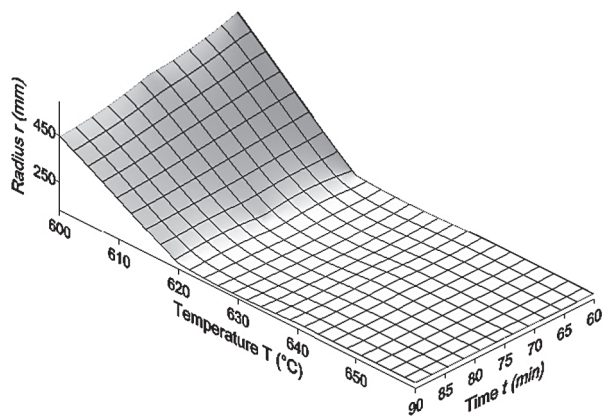


Figure 6. Radius of glass foil shape as a function of temperature and time formed by the free slumping.

you can see in Figures 10 and 11. The micro-roughness  $R_a$  measured with ZYGO or AFM was around 0.3 nm. The surface of the foils shaped by the free slumping, measured with the mechanical profilometer, had  $R_a$  also about 0.3 nm.

We successfully shaped the silicon foils by hot plastic deformation, and thus, confirmed again the feasibility of this process. We used cylindrical pressing mandrels with radius from 10 to 75 mm as well as spherical mandrels of radius 30 mm. By changing heat-treatment conditions and the geometry of a pressing mandrel, we were able to form silicon foils with various curvatures; for example, the foils with radius 252, 398, and 47 mm are shown in Figures 12 to 15. Using AFM, we measured the surface micro-roughness of Si foils before

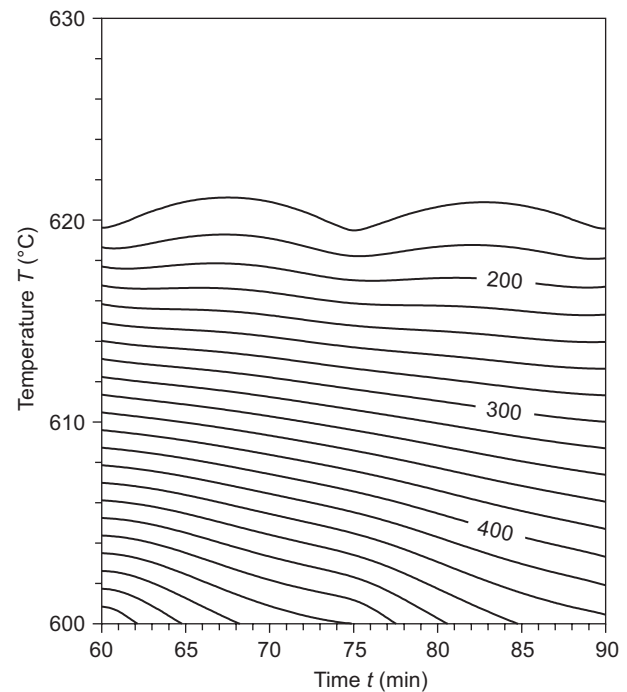


Figure 7. Radius isolines of glass foil shape as a function of temperature and time formed by the free slumping.

and after their shaping. Their original micro-roughness  $R_a$  only slightly increased from 0.07 to 0.1 nm. In Figure 16, you can compare the images of the original Si foil and of the thermally shaped one.

DISCUSSION

In the forming experiments, we compared the shapes of glass foils formed by free or forced slumping. The obtained shapes were close to parabola but it was also possible to fit them with circle with reasonably low deviations characterized by peak-to-valley values below

36  $\mu\text{m}$ . However, we are still continuing our effort to decrease these values to the micrometre region by optimizing the forming process. By this approach, we could use the radius as just one parameter to characterize the shape. For free slumping, we observed that at temperatures above roughly 620°C, i.e., at  $\eta = 10^{10.5}$  dPa-s, the glass foil's shape did not significantly change with  $T$  and  $t$ . The sagging velocity was high enough for the foil to reach the top surface of the mandrel and rest on it. The foils' radii were in the range of 130-150 mm, that is a little bit higher than the mandrel's radius  $r = 122.3$  mm, indicating more open shape. On the other hand, below 620°C, the shape was strongly

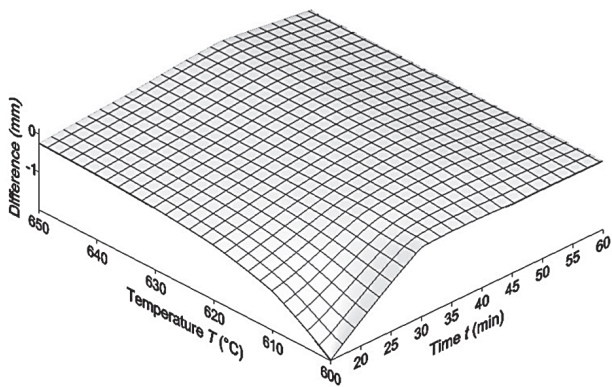


Figure 8. Shape radius difference between a glass foil and the mandrel as a function of temperature and time for forced slumping.

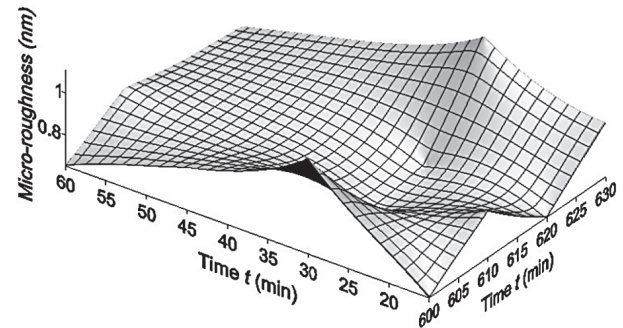


Figure 10. Surface micro-roughness, measured with mechanical profilometer, of glass foils formed by forced slumping as a function of temperature and time.

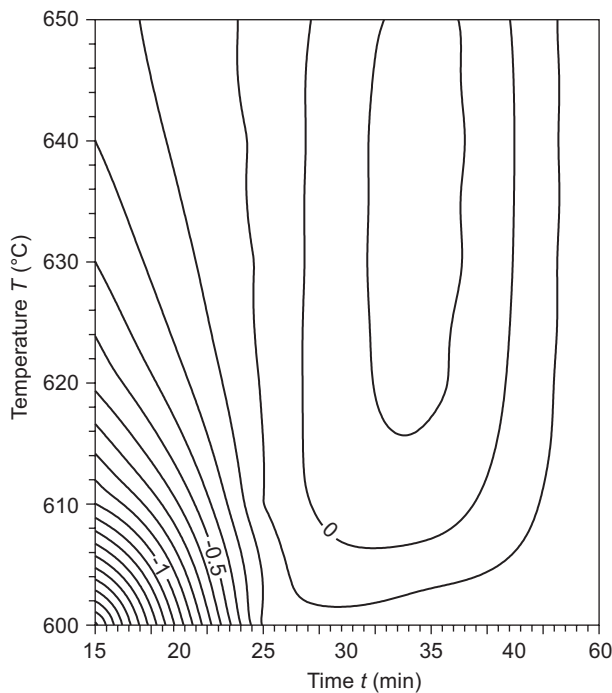


Figure 9. Isolines of shape radius difference between a glass foil and the mandrel as a function of temperature and time for forced slumping.

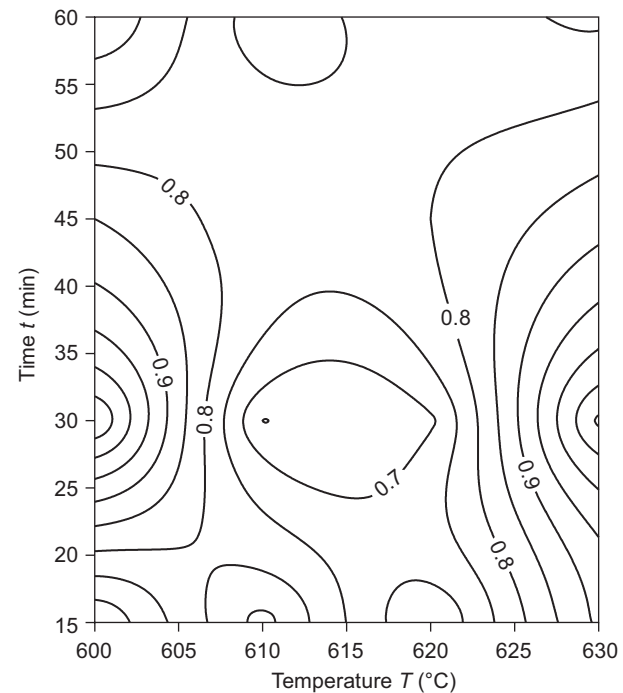


Figure 11. Isolines of constant surface micro-roughness, measured with mechanical profilometer, of glass foils formed by forced slumping as a function of temperature and time.

dependent on  $T$  and also quite significantly dependent on  $t$ . At these temperatures, the sagging glass foil did not reach the mandrel surface and the resulting shape was much more open with radii spanning from 150 to 590 mm. For forced slumping, we put a pressing mandrel on the top surface of the glass foil, which significantly speeded up the sagging. The glass foils almost always reached the mandrel's surface. Thus, the foils' radius was found to be very close to the radius of the mandrel. The map with the differences contains a zero isoline that marks the temperature-time area where we can obtain the radius of the foil to be the same as, of the mandrel. Only in a small area below 620°C and  $t$  shorter than 30 min, the radius was steeply decreasing with the decreasing  $T$  and  $t$ .

Our measurements with the profilometer revealed that the micro-roughness of glass foils' surfaces was strongly dependent on  $T$  and  $t$  when the foils were formed by the forced slumping. The 3-D plot and the corresponding map indicate the temperature-time area where we achieved the  $R_a$  values to be below 0.7 nm.

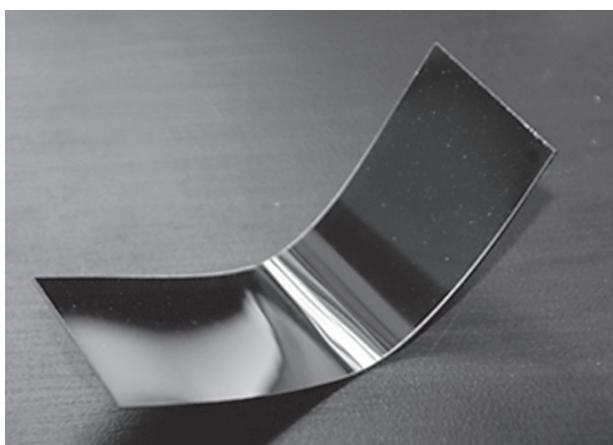


Figure 12. Si foil of radius 252 mm shaped by hot plastic deformation.

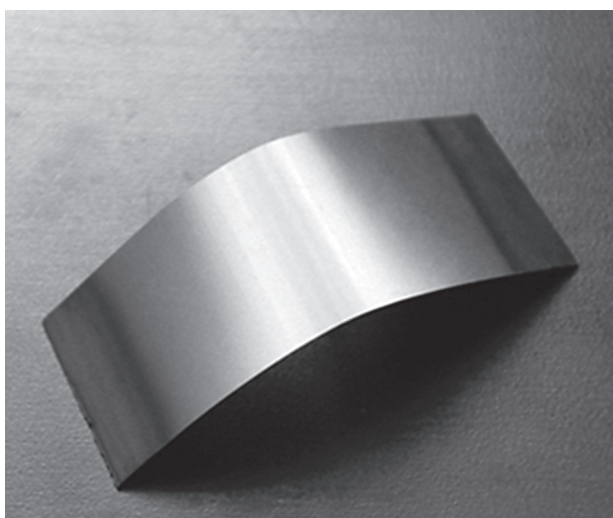


Figure 13. Si foil of radius 398 mm shaped by hot plastic deformation.

This area is approximately between 610 and 620°C with  $t$  between 25 and 35 min. The upper pressing mandrel could significantly affect the foil's surface quality when the forming conditions are not optimal. The measurements of the foils' surface using ZYGO and AFM determined  $R_a$  to be much lower, only 0.3 nm. The data obtained from the profilometer were probably affected by the waviness of the samples. For the free slumping, the measurements with profilometer determined the  $R_a$  values to be about 0.3 nm. It is probable that the untouched surface of these glass foils had significantly better smoothness.

During the forming experiments, we proved that the composite mandrel is suitable for the thermal forming of glass foils for the mirrors of x-ray space telescopes. The composite material prevents sticking of glass to the mandrel at high temperatures, and the manufacture of the mandrel is simple and cost-effective.

By controlling  $T$  and  $t$  in a particular temperature-time area, we could also prepare foils with various radii, and hence, use just one mandrel for manufacturing different mirror reflectors. This approach could also significantly lower the production cost of x-ray telescopes mirrors.

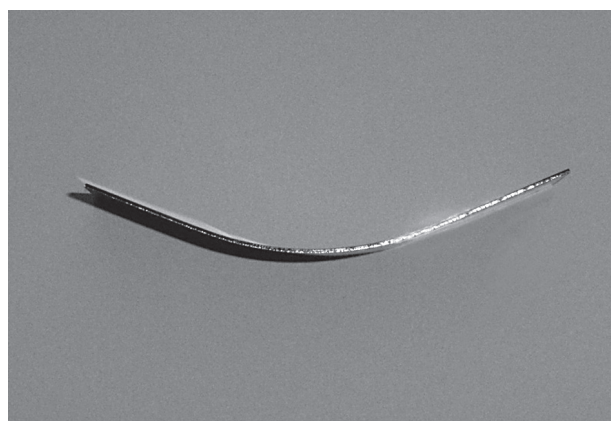


Figure 14. Si foil of radius 47 mm shaped by hot plastic deformation.

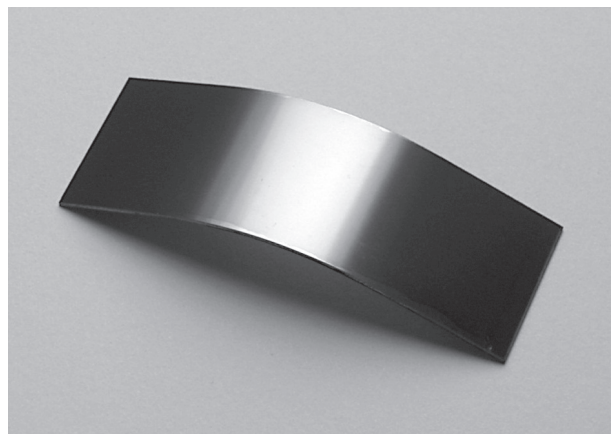


Figure 15. Si foil of radius 47 mm shaped by hot plastic deformation.

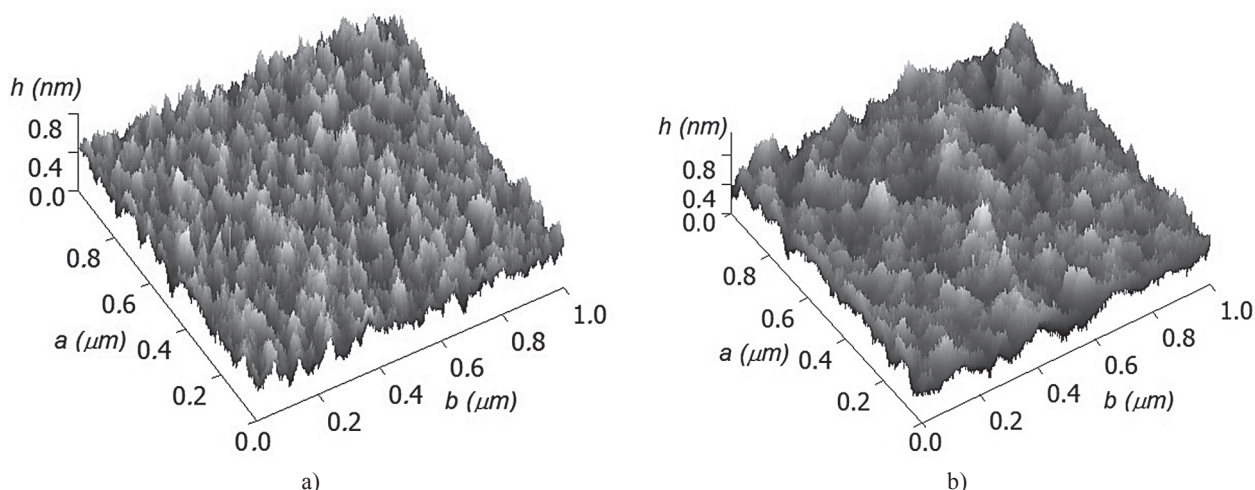


Figure 16. AFM images of a silicon foil surface before (a) and after the thermal forming process.

In our experiments, we confirmed that thin silicon foils can be effectively shaped by the thermal forming process. However, the process is complex, and to successfully shape the foils, we need to use wafers with sufficient concentration of dislocations with proper orientation. To achieve sufficient bending, we had to heat up the foils above 1000°C, to the region of plastic deformation, where the dislocations move in a viscous manner, and keep them at high temperature for more than 60 min. By using the pressing mandrels of different geometry; for example cylinders or spheres of various radii, and by controlling heat-treatment conditions, we could form the foils to required shapes. However, the precise shaping of the foils at such high temperatures turned to be a highly demanding process.

## CONCLUSION

We compared the shapes of glass foils thermally formed by free or forced slumping in our composite mandrel. The obtained shapes were fitted with a circle. The free slumping process formed shapes with bigger radii than the radius of the mandrel. At temperatures below 620°C, the radius strongly increased with the decreasing temperature and time of heat-treatment. The forced slumping formed shapes with radii very close to the mandrel. We defined the time-temperature area where these radii are the same. The samples formed by the free slumping had lower micro-roughness than those formed by the forced slumping.

By controlling  $T$  and  $t$  in a particular temperature-time area, we could also prepare foils with various radii and sufficiently low micro-roughness, and hence, use just one mandrel for manufacturing different mirror reflectors. This approach could also significantly lower the production cost of x-ray telescopes mirrors.

Thin silicon foils could be effectively shaped by force in the region of hot plastic deformation if they contain the sufficient concentration of properly oriented dislocations. To facilitate the movement of dislocations, the foils had to be heated above 1000°C for longer than 60 min. The highly smooth surface of the foils was not significantly deteriorated by the thermal forming process. However, the precise shaping of silicon at high temperatures turned out to be a highly demanding process. Nevertheless, we still consider the silicon optics to be a very promising technology for lightweight and high-resolution x-ray imaging telescopes.

## Acknowledgment

*M. Mika thanks D. Cerna for her AFM and profilometer measurements. Authors thank for the support of the Grant agency of the Academy of Sciences of the Czech Republic "Material and X-Ray Optical Properties of Formed Silicon Monocrystals," IAAX01220701; and the research program MSM 6046137302 "Preparation and research of functional materials and material technologies using micro- and nanoscopic methods".*

## References

1. Wang Q.D., Gotthelf E.V., Lang C.C.: *Nature* 415, 148 (2002).
2. Stage M.D., Allen G.E., Houck J.C., Davis J.E.: *NatPh* 2, 614 (2006).
3. Hickox R.C., Jones C., Forman W.R., Murray S.S., Brodwin M., Brown M.J.I., Eisenhardt P.R., Stern D., Kochanek C.S., Eisenstein D., Cool R.J., Jannuzi B.T., Dey A., Brand K., Gorjian V., Caldwell N.: *ApJ* 671, 1365 (2007).

4. Giacomini, R., Zirm, A., Wang, J., Rosati, P., Nonino, M., Tozzi, P., Gilli, R., Mainieri, V., Hasinger, G., Kewley, L., Bergeron, J., Borgani, S., Gilmozzi, R., Grogin, N., Koekemoer, A., Schreier, E., Zheng, W., Norman, C.: *ApJS* 139, 369-410 (2002).
5. Luo B., Bauer F.E., Brandt W.N., Alexander D. M., Lehmer B.D., Schneider D.P., Brusa M., Comastri A., Fabian A. C., Finoguenov A., Gilli R., Hasinger G., Hornschemeier A. E., Koekemoer A., Mainieri V., Paolillo M., Rosati P., Shemmer O., Silverman J.D., Smail I., Steffen A.T., Vignali C.: *ApJS* 179, 19 (2008).
6. <http://ixo.gsfc.nasa.gov>
7. Zhang W.W., Atanassova M., Augustin P., Blake P.N., Byron G., Carnahan T., Chan K. W., Fleetwood C., He C., Hill M.D., Hong M., Kolos L., Lehan J.P., Mazzarella J. R., McClelland R., Olsen L., Petre R., Robinson D., Russell R., Saha T.T., Sharpe M., Gubarev M.V., Jones W.D., O'Dell S.L., Davis W., Caldwell D.R., Freeman M., Podgorski W.A., Reid P.B.: *Proc. SPIE* 7437, 0Q:1-12 (2009).
8. Ghigo M., Basso S., Bavdaz M., Conconi P., Citterio O., Civitani M., Friedrich P., Gallieni D., Guldemann B., Martelli F., Negri R., Pagano G., Pareschi G., Parodi G., Proserpio L., Salmaso B., Scaglione F., Spiga D., Tagliaferri G., Terzi L., Tintori M., Vongehr M., Wille E., Winter A., Zambra A.: *Proc. SPIE* 7732, 0C:1-12 (2010).
9. Hudec R., Sik J., Lorenc M., Pina L., Marsikova V., Mika M., Inneman A., Skulinova M.: *Proc. SPIE* 8076, 807604, 2011.
10. Hudec R., Pina, L., Marsikova, V., Inneman, A., Skulinova, M., Mika, M.: *AIP Conf. Proc.*, vol. 1248, pp. 587–588, 2010.
11. Ezoe Y., Shirata T., Ohashi T., Ishida M., Mitsuda K., Fujiwara K., Morishita K., Nakajima K.: *Proc. SPIE* 7360, 0B:1-8 (2009).
12. Wallace K., Bavdaz M., Gondoin P., Collon M. J., Guumlnther R., Ackermann M., Beijersbergen M.W., Olde Riekerink M., Blom M., Lansdorp B., de Vreede L.: *Proc. SPIE* 7437, 0T:1-9 (2009).
13. Collon M.J., Günther R., Ackermann M., Partapsing R., Vacanti G., Beijersbergen M. W., Bavdaz M., Wille, E., Wallace K., Olde Riekerink M., Lansdorp B., de Vreede L., van Baren, C., M&uuml;ller, P., Krumrey, M., Freyberg, M.: *Proc. SPIE* 7732, 1F:1-9 (2010).
14. Wolter H.: *AnP* 445, 94 (1952).
15. Hudec R., Pina L., Semencova V., Inneman A., Skulinova M., Sveda L., Mika M., Brozek V., Kacerovsky R., Prokop J., Sik J.: *Nuclear Physics B* 166, 258 (2007).
16. Hudec R., Marsikova V., Mika M., Sik J., Lorenc M., Pina L., Inneman A., Skulinova M.: *Proc. SPIE* 7437, 0S:1-12 (2009).
17. Prosperio L., Civitani M., Ghigo M., Pareschi G.: *Proc. SPIE* 7803, 0K:1-11 (2010).
18. [www.us.schott.com/special\\_applications/english/products/thinglass/d263t/index.html](http://www.us.schott.com/special_applications/english/products/thinglass/d263t/index.html).
19. Nakajima K., Fujiwara K., Morishita K.: *J. Cryst. Growth* 311, 4587 (2009).
20. Nakajima, K., Fujiwara, K., Pan, W., and Okuda, H.: *Nature Materials* 4, 47 (2005).